REGULAR PAPER

Thermal Analysis of 3J33 Grinding Under Minimum Quantity Lubrication Condition

Zishan Ding[1] · Jian Sun[1] · Weicheng Guo[1] · Xiaohui Jiang[1] · Chongjun Wu[2] · Steven Y. Liang[3]

Abstract

With the increasing requirements of environmental protection, energy conservation, and low consumption, minimum quantity lubrication (MQL) technology has attracted people's attention. In the grinding process, the cooling performance of MQL has always been the focus. In this study, considering the influence of the grinding wheel speed, grinding fluid flow rate, and gas pressure on the useful flow rate, the MQL grinding cooling performance was studied and analyzed, and the MQL grinding heat transfer coefficient model, grinding energy partition model and grinding temperature calculation model were established. Grinding experiments were carried out with maraging steel 3J33 as the experimental object, of which the results verified the accuracy of the model. The error of temperature calculation model is 9.45%. The influence of different parameters on the surface processing quality of the workpiece was studied through experimental results. The results show that the grinding wheel speed and gas pressure have a more significant influence on the useful flow rate of the grinding fluid. The grinding fluid flow rate but significant impact on the surface quality of the workpiece.

✉ Weicheng Guo
wcguo@usst.edu.cn

Zishan Ding
zishanding1988@gmail.com

Jian Sun
sunjian4113@163.com

Xiaohui Jiang
jiangxh@usst.edu.cn

Chongjun Wu
wcjunm@dhu.edu.cn

Steven Y. Liang
steven.liang@me.gatech.edu

1   College of Mechanical Engineering, University of Shanghai for Science and Technology, 330, Mechanical Engineering Academic Building, 516 Jungong Road, Shanghai 200093, China

2   College of Mechanical Engineering, Donghua University, Shanghai 200093, China

3   George W. Woodruff School of Mechanical Engineering, Georgia Institute of Technology, Atlanta 30332, USA

1 Instruction

In recent years, with the deepening of the application of aerospace engineering, higher requirements are raised to obtain high performance and high-degree control of the manufacturing process. Grinding has become one of the most widely used processing methods to achieve the required quality and meet the requirements of high-quality parts [1–5]. During grinding, many of the abrasive grits are in contact with the work piece each second, but only a portion of these grits play the cutting role in the real process, and the others do not participate in the real cutting, but generate heat by rubbing and ploughing the work piece surface in the grinding contact zone [6, 7]. High heat generation and temperature in the grinding contact zone are associated with a high negative rake angle, and with a great contact length in grinding process [8, 9]. The heat disperses to the grinding ship, wheel, and work pieces. However, only a small proportion of grinding heat is removed by abrasive dust, and most heat is transferred to work pieces, which may lead to various types of thermal damage to the work piece, such as burning, phase transformations, unfavorable residual tensile stresses, and cracks [10–13]. Sun et al. [14] found that the temperature rise could cause the transformation of the material

microstructure. Xi et al. [15] analyzed the effect of grinding temperature on the properties of heat affected zone on the surface of work piece materials, and pointed out that high grinding temperature will introduce more residual tensile stress. Therefore, to ensure the performance and quality of the work pieces, the grinding temperature must be under control. In general, flood grinding fluid is used to reduce the grinding force and the grinding temperature. However, the extensive use of cutting fluid will also bring environmental problems, and greatly increase the processing cost. Moreover, a number of researches show that the dry grinding has higher grinding force, grinding temperature, surface roughness and longer wheel life than overflow cooling [16]. Grinding with insufficient grinding fluid may result in defects, such as thermal damages and dimensional inaccuracies, besides, dry grinding fail to achieve successful yield results [17].

A promising alternative to dry grinding and flood grinding fluid lies in MQL grinding which requires only a small amount of grinding fluid, therefore, it is regarded as a kind of near-dry grinding. According to the experiments, MQL technology can be of great help to the reduction of grinding force, grinding temperature and surface quality [16, 18–23]. This is because that under the action of compressed gas makes it easier for the grinding fluid to pass through the air boundary layer around the grinding wheel to reach the grinding area [8, 24].

Grinding temperature has a key influence on the quality of work piece, and a considerable research effort has been made to both theoretical and experimental aspects of heat transfer in grinding. Due to the random distribution of grits on the wheel, the grinding force is periodic. Accordingly, the heat flux into the work piece is not continuous as a function of both location and time. Hamid Jamshidia and Erhan Budak [25] established a temperature prediction model base on a time dependent heat source. It can be seen from the experiment result that the temperature predicted is within the range from 10–15 °C which is higher than the experimental temperature. Ding et al. [26] conformed that the new model is more appropriate for the analysis of grinding energy partition. In this model, the velocity of the work piece was considered.

However, for the thermal analysis of MQL grinding, the traditional thermal models are not enough. There are many factors with an impact on the distribution of MQL grinding temperature. Sharmin et al. [27] designed a modified nozzle, and found that lower temperature could be observed by the modified nozzle. Studies show that the type of grinding fluid and additives will also affect the cooling performance of MQL and the surface temperature of the work piece [28–30]. The convective heat transfer of MQL jet will impact the distribution of grinding heat. And it is necessary to consider the character of MQL jet when investigating the grinding temperature of MQL grinding. Hadad and Sadeghi [31] proposed a model of heat distribution which considered the effect of the MQL jet. Based on this point and the moving triangular heat source model, a temperature prediction model was created, in which the MQL jet is deemed as a homogeneous two-phase fluid with equal liquid and gas velocities and temperatures in the flow cross-sectional area. However, under the action of the viscous force, the droplets will attach to the surface of the work piece, and separate from the compressed air. Therefore, in the grinding region, the MQL jet should not be regarded homogeneous two-phase fluid. Li et al. [32] investigated the effect of nanofluid minimum quantity lubrication (MQL) on the temperatures in surface grinding, and proposed a model for convective heat transfer coefficient based on the boundary layer theories.

It can be found from the literature review that the thermal analysis of MQL grinding is not enough. In this article, the MQL jet in the grinding zone will be considered as two parts, i.e., the compress air and cooling droplets. Besides, the heat transfer coefficient of compress air and cooling droplets was calculated separately. On this basis, a temperature rise model of grinding was established. Due to the air boundary around the wheel, not all the cooling droplets can enter into the grinding zone. The "useful flow rate" model was established, based on which the convection heat transfer coefficient of MQL grinding model was constructed. In this manner, the grinding heat partition ratio could be calculated more accurately. However, in the existing literatures, there were few studies on the construction of MQL grinding heat calculation model based on the consideration of the effective flow of grinding fluid. In this study, the surface grinding experiment of 3J33 was carried out. The surface temperature of the work piece was measured by thermocouple to verify the correctness of the temperature rise model and the calculation of heat distribution ratio. According to the experiment results, the influence of MQL grinding parameters on surface quality was analyzed.

2 Theoretical Thermal Model of MQL Grinding

In this section, the grinding thermal analysis of grinding under the condition of MQL was developed based on the existing grinding thermal analysis. In the modeling, the effect of MQL on grinding heat distribution was considered. During the MQL grinding process, the heat generated in the grinding zone is transferred into wheel, chip, and workpiece, while a part of heat in the workpiece flows into the MQL jet. The heat distribution in grinding zone is shown as Fig. 1.
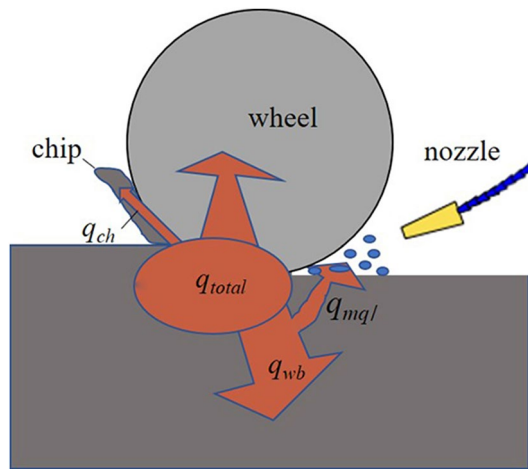
Fig. 1 Grinding heat distribution

2.1 Energy Partition Analysis

There are three stages in the grinding process: sliding, ploughing and cutting. In sliding and ploughing, the friction at wheel/chip and wheel/workpiece interface will produce a lot of heat. Moreover, the plastic deformation of the workpiece surface under the action of extrusion pressure will also produce a lot of heat. These two stages are the root source of grinding heat. The heat generated during grinding will be transferred to chip, wheel, workpiece and grinding fluids, which can be expressed as:

$$q = q_{ch} + q_w + q_s \tag{1}$$

where q is the total heat flux generated in grinding zone, q_{ch} is the heat flux to chip, q_s is the heat flux to wheel, q_w is the heat flux to workpiece MQL oil mist.

The average heat flux density in the grinding area can be calculated as:

$$q = \frac{F_t v_s}{l_c b} \tag{2}$$

$$l_c = \sqrt{a_p.d_s} \tag{3}$$

where F_t is tangential grinding force, v_s is the grinding wheel speed, l_c is the contact length, b is the grinding width, a_p is the grinding depth and d_s is the grinding wheel equivalent diameter.

The ratio of heat flux distribution to chip can be estimated by the total heat flux generated in the grinding zone and the heat flux taken by the chip. The heat partition to the chip can be expressed as:

$$R_{ch} = \frac{q_{ch}}{q} \tag{4}$$

The heat flux transferred to chips can be estimated as [29]:

$$q_{ch} = e_{ch}\frac{a_p v_w}{l_c} = \frac{a_p v_w}{l_c} \tag{5}$$

where v_w is the moving rate of the heat flux and corresponds to the workpiece feed rate.

The limiting chip energy can be expressed as:

$$e_{ch} = \rho_w c_w T_{mp} \tag{6}$$

where ρ_w is the density of workpiece material, c_w is the specific heat capacity, and T_{mp} is the melting point temperature of workpiece material.

The heat flux in the workpiece is the key factor that affects the temperature rise of workpiece in the grinding zone. Under the condition of MQL, the MQL jet will take away a lot of heat, so the convective heat transfer of MQL must be taken into account when calculating the heat flux flowing into the workpiece. The heat flux transferred into the workpiece and lubricant can be estimated as [33]:

$$q_w = \frac{kv_w^{0.5}}{\beta\alpha_w^{0.5}a_p^{0.25}d_s^{0.25}}T_{max} \tag{7}$$

where k is the thermal conductivity, β is a constant which depends on the shape of heat source ($\beta = 1.06$ for the triangular distribution heat source), α_w is the thermal diffusivity of workpiece material, and T_{max} is the maximum temperature at the grinding zone which can be measured by thermal couple.

The heat partition to workpiece and grinding fluid can be expressed as:

$$R_w = \frac{q_w}{q} \tag{8}$$

The MQL jet mainly takes away the heat from the grinding zone in the form of convective heat transfer, and the heat flux that transfers to the MQL oil mist can be calculated as:

$$q_{mql} = h(T_0 + T_e - T_{in}) \tag{9}$$

and the heat partition to MQL oil mist can be expressed as:

$$R_{mql} = \frac{q_{mql}}{q} \tag{10}$$

where h is the convection heat transfer coefficient of MQL jet, T_0 is the temperature rise of workpiece, T_e is the ambient temperature (25 °C), and T_{in} is the initial temperature of MQL oil mist.

The heat flux in workpiece can be calculated as:

$$q_{wb} = q_w - q_{mql} \tag{11}$$

The heat partition in workpiece can be expressed as:

$$R_{wb} = \frac{q_{wb}}{q} \tag{12}$$

Thus, heat partition in wheel is:

$$R_s = 1 - R_{ch} - R_{wb} - R_{mql} \tag{13}$$

2.2 The Convection Heat Transfer Coefficient of MQL

As discussed above, a part of the heat generated in the grinding zone is transferred to MQL. In order to determine the heat flux transferred to the MQL, the convection heat transfer coefficient of the MQL must be calculated. After the MQL jet passes through the air boundary layer to the grinding zone, under the action of viscous force, most of the droplets attach to the surface of the workpiece, and only a few of the droplets will be dispersed in the compressed gas. Compared with the material flow rate of compressed gas, the droplets dispersed in compressed gas can be ignored. When calculating the heat transfer coefficient of MQL in grinding zone, the convective heat transfer coefficient of compressed gas and the convective heat transfer coefficient of droplets can be considered separately.

When the effect of droplets is not considered, based on the theory of conduction of heat, the convection heat transfer coefficient of gas flow can be calculated as:

$$h_a = \frac{kN_u}{l_c} \tag{14}$$

$$N_u = 0.706 P_r^{1/3} R_e^{1/2} \tag{15}$$

where Re is the Reynolds number, P_r is the Prandtl number and N_u is the Nusselt number; $Re = v_g \rho_g l_c / \mu_g$, $Pr = \mu_g C_p / k_g$. Where ρ_g is the density of gas flow, v_g is the average velocity of gas flow, μ_g is the dynamic viscosity of gas, C_p is the specific heat capacity of air.

The droplets entering the grinding zone are attached to the surface of the workpiece under the action of viscous force, and the droplets are spread out on the surface of the workpiece (see Fig. 2).

The spreading area can be calculated as:

$$A = 1/4\pi D^2 \tag{16}$$

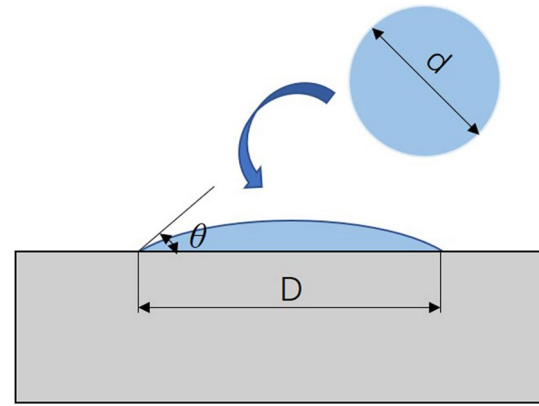The diameter of spreading area can be calculate as [34]:

Fig. 2 Droplet spread on the surface

$$D = \sqrt[3]{\frac{V}{\frac{\pi}{2} \frac{1}{tan\theta} \left(\frac{1}{cos\theta} - 1 \right) \left[1 + \frac{1}{3tan^2\theta} \left(\frac{1}{cos\theta} - 1 \right)^2 \right]}} \tag{17}$$

$$V = \frac{4}{3}\pi \left(\frac{d}{2} \right)^3 \tag{18}$$

where θ is contact angle. For the single droplet, the convection heat transfer coefficient can be calculated as:

$$h_s = \frac{C_l \rho_l V}{A} \tag{19}$$

where C_l is the specific heat capacity of grinding fluid. Then the total convection heat transfer coefficient of MQL oil droplet can be expressed as:

$$h_l = \frac{Q'}{V} h_s \tag{20}$$

where Q' is the flow rate of grinding fluid which penetrate into grinding zone, V is the volume of grinding fluid droplet.

Therefore, the convection heat transfer coefficient of MQL can be expressed as:

$$h = h_a + h_l \tag{21}$$

2.3 Grinding Temperature Model

Based on the moving heat source theory, uniform rectangular heat source model assumes two-dimensional heat transfers in the x–z plane with uniform rectangular heat source distribution on the workpiece surface along the contact zone. The heat distribution is uneven with the increase of grinding depth. Triangular heat source model assumes a triangular heat source distribution in grinding zone (Fig. 3). When both models predict only slight differences for the same average heat flux at the contact zone, the temperature response with
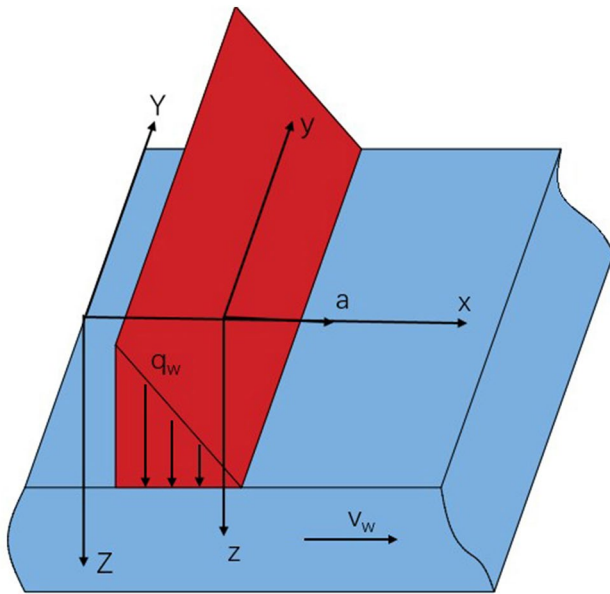
Fig. 3 Moving triangular heat source on the surface

the triangular distribution has been found to be more consistent with measured temperature profiles. For this moving heat source model, the temperature rise in the workpiece is given by [35]:

$$
T_0(x,z) = \frac{q_{wb}}{\pi k_w} \int_{-l_c/2}^{l_c/2} e^{-\left(v_w(x-a)/2\alpha\right)} \\
\times K_0 \left\{ \frac{v_w}{2\alpha_w} \left[(x-a)^2 + z^2 \right]^{\frac{1}{2}} \right\} f(a) da
$$

(22)

where for triangular heat source distribution:

$$
f(a) = 1 + (2a/l_c)
$$

(23)

2.4 Useful Flowrate

In the grinding process, the total rotation of the grinding wheel will form an air barrier layer around the grinding wheel and produce backflow in the wedge zone formed between the grinding wheel and the workpiece, which will prevent the grinding fluid from entering the grinding zone. And part of the droplets in the MQL jet will be suspended in the air, which does not play the role of cooling and lubrication. Therefore, only a part of the grinding fluid ejected by MQL enters the grinding zone and plays the role of cooling and lubrication. This part of the grinding fluid is called effective grinding fluid. The ratio of the flow Q' to the total flow Q is the useful flow rate ratio ξ

$$
\xi = \frac{Q'}{Q}
$$

(24)

The useful flow rate of grinding fluid is mainly affected by grinding wheel speed, gas pressure and grinding fluid flow rate. In order to obtain the useful flow rate, the surface grinding temperatures under different conditions were measured.

3 Experiment Procedure

3.1 Parameters Detection

3.1.1 Contact Angle Test

After the grinding fluid reaches the surface of the workpiece, it will adhere to the surface of the workpiece and spread out. Due to the surface tension of the droplet, the droplet cannot fully spread out on the surface of the workpiece, and will form a certain angle with the surface of the workpiece, which is called contact angle. The value of the contact angle reflects the wetting performance of the grinding fluid. The smaller the contact angle, the larger the wetting area and the better the heat transfer performance. In this study, a contact angle measuring instrument was used to measure the contact angle, as shown in Fig. 4.

3.1.2 Droplet Size Test

According to the atomization theory, the size of the spray droplets is different, and they are distributed regularly. In this study, the Sauter average diameter D32 was used to characterize the MQL spray droplets. Malvern laser particle size analyzer was used to measure the average diameter of MQL spray under different parameters. The model of the instrument is LDSA-SPR 1500A. The physical picture of the measurement system is shown in Fig. 5. The test result is shown in the Table 1.

3.2 Grinding Experiment

In this study, a Carver S600A machine tool was used for surface grinding experiments. The maximum speed of the machine tool spindle is 18000 rpm, and the maximum working stroke of the x, y and z axes are 600 mm, 500 mm, and 300 mm. The grinding wheel used in the grinding experiment is a CBN grinding wheel. The size of the workpiece in the grinding experiment is 15 mm×15 mm×70 mm, and the workpiece material is maraging steel 3J33. The main components and material properties are shown in Tables 2 and 3.

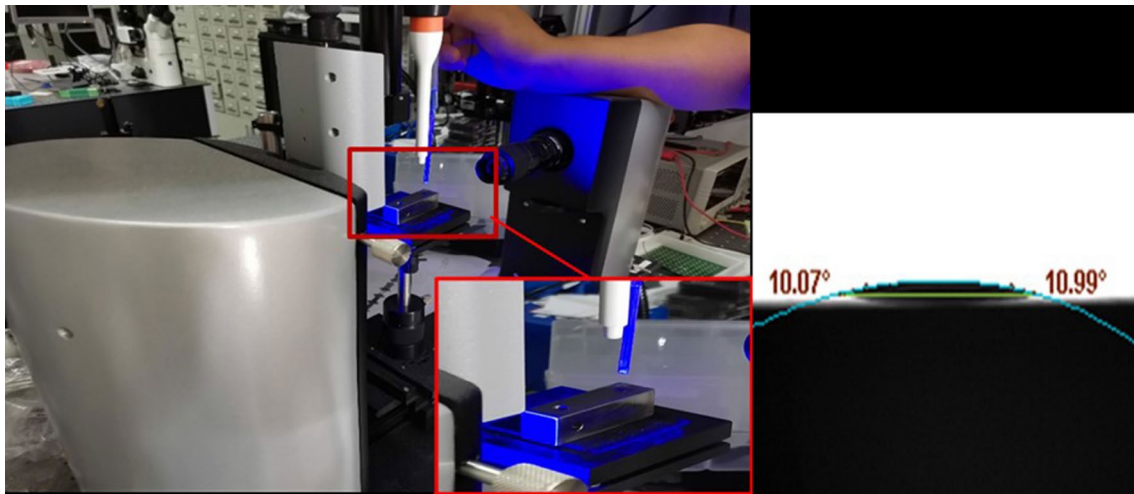The workpiece was connected to the German Kistler-9139A three-dimensional dynamometer through a
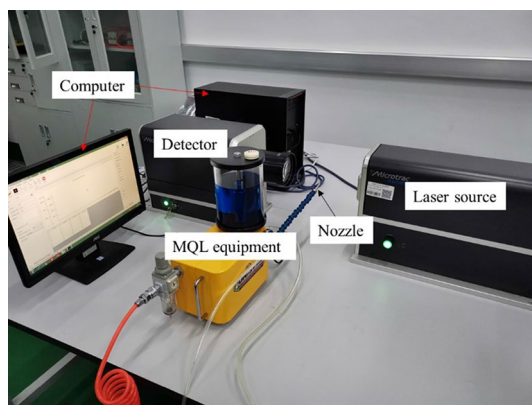
Fig. 4 Contact angle test

Fig. 5 Droplet size test equipment

rectangular parallelepiped steel plate to measure the grinding force during the grinding process. A NI-9351 thermometer was used to connect the K-type thermocouple with the LAB view signal acquisition system to measure the grinding temperature of the workpiece surface. A green silicon carbide oil stone was used for dressing the grinding wheel after

measuring each group of parameters in the grinding experiments. The UNI-MAX MQL equipment was used during the grinding process with vegetable oil. The material properties of vegetable oil are shown as Table 4. The experiment equipment is shown as Fig. 6.

As shown in Fig. 7, the workpiece was divided into two parts. There is a groove at the end of workpiece, and the thermocouple is placed in the groove. The thermocouple wire was clamped between Workpiece 1 and workpiece 2 which were connected by screws. In addition, polyimide film was used for insulation and isolation between the two poles of the thermocouple and between the thermocouple and the workpiece. During the grinding process, due to the high temperature generated in the grinding zone and the squeezing effect of the grinding wheel, the thermocouple is connected by insulated and isolated two poles and welded to form a thermocouple node, thereby forming a closed loop and realizing the measurement of the grinding temperature.

The cooling and lubrication effect of MQL is better when the MQL nozzle is positioned angularly toward the wheel (at approximately 10°–20° to the workpiece surface) [5]. Therefore, in the experiment, the values of nozzle angle

Table 1 The test result of droplet SMD diameter (μm)

	30.12 mL/h	35.77 mL/h	41.53 mL/h	54.11 mL/h	66.41 mL/h	77.17 mL/h
2 bar	66.35	63.82	73.51	65.22	62.078	59.61
4 bar	30.54	28.31	30.57	28.95	35.47	43.61
6 bar	22.43	22.13	24.12	24.20	25.39	26.98

Table 2 Chemical composition (wt%) of 3J33 maraging steel

Fe	Al	Co	Mn	Ni	Si	Ti	P	C	S
71.766	0.09	8.98	0.02	18.45	0.03	0.65	0.003	0.01	0.001

Table 3 Material properties for maraging steel 3J33

Parameters	Description	Values
E_m	Modulus of elasticity	1.9E5 MPa
v_p	Poisson's ratio	0.3
ρ	Density	7830 kg/m^3
C_h	Specific heats	477 J/kg °C
K_h	Thermal conductivities	25.3 W/m °C
K_t	Thermal linear coefficient	10.6E−6
T_{mp}	Melting temperature	*1723 K*
HV	Vickers hardness	265 HV

Table 4 Material properties for vegetable oil

Parameters	Description	Values
k_f	Thermal conductivity	0.1744 (W/(m · K))
C_f	Specific heats	2352 (J/(Kg ·°C))
ρ_f	Density	0.856 (g/mL)
μ	Kinematic viscosity	42.38 (mm^2/s)
σ	Surface tension coefficient	29.407 (mN/m)

and droplet deposition distance are taken as 15° and 40 μm, respectively. The cooling and lubrication effect of MQL mainly depends on the ability of the grinding fluid to penetrate the air boundary and enter the grinding zone, which is mainly related to the gas pressure P, the flow rate of the grinding fluid Q and the wheel speed v_s. The workpiece feed rate v_w and grinding depth a_e mainly affect the heat in the

grinding zone, and have almost no effect on the penetration of the grinding fluid through the air boundary layer. Therefore, in the experiment, the feed speed and grinding depth are taken as fixed values, which are 0.01 m/s and 8 μm, respectively. Other experimental parameters are shown in Table 5.

In order to study the influence of MQL cooling on the surface processing quality of the workpiece, the Form Talysurfi 200 roughness meter (Fig. 8a) and 9XF transmission reflection metallographic microscope (Fig. 8b) were used to detect the surface roughness and surface morphology of the workpiece under different experimental conditions, and the residual stress was detected by PROTO X-ray stress analyzer (Fig. 8c), the equipment parameter settings are shown in the Table 6.

4 Results and Discussion

4.1 The Result of Grinding Heat Participation

The grinding heat distribution is the prerequisite for the calculation of the grinding temperature. To study the effect of the useful flow of the MQL grinding fluid on the heat flowing into the workpiece, the grinding heat flowing into the workpiece under the useful flow and without the useful flow is calculated with the result shown in Fig. 9. Through the comparison of the calculation results in the figure, it was found that the grinding heat distribution ratio calculated by considering the useful flow rate of the MQL grinding fluid

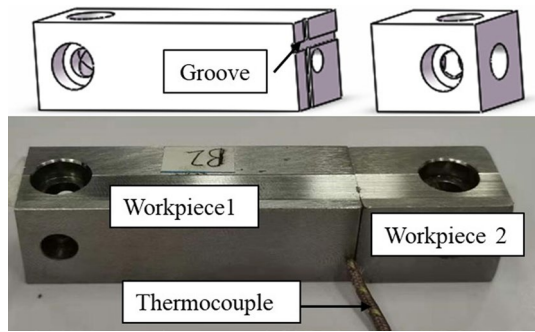**Fig. 6** Grinding experimental setup

Fig. 7 Schematic diagram of thermocouple installation

Table 5 Parameters of experiment

Wheel rotation speed (v_s)	v_s = 20, 25, 30, 35, 40 m/s
Feed speed (v_w)	v_w = 0.02 m/s
Cutting depth (a_e)	a_e = 8 μm
MQL flow rate (Q)	Q = 35.77, 41.53, 54.11,66.41,77.17 mL/h
MQL pressure (P)	P = 2, 3, 4, 5, 6 bar

is higher than that without the consideration of the useful flow rate of the grinding fluid by an average value of 15.8%. Due to the grinding process, part of the grinding fluid fails to enter the grinding area under the action of the flow field of the grinding wheel, which cannot be effectively cooled, resulting in an increase in the grinding heat entering the workpiece. In this case, the useful flow rate of the grinding fluid must be considered when calculating the grinding heat distribution.

4.2 The Result of Useful Flow Rate Ratio

According to the data obtained from the experiment, when substituting it into the model in Sect. 2, the useful flow rate of the grinding fluid under different experimental conditions are obtainable. The calculated results of different parameters are shown in Fig. 10a–c.

It can be seen from Fig. 10a that the grinding fluid flow rate has little effect on the useful flow rate of the grinding fluid which hardly changes with the flow rate of the grinding fluid. This is because that the grinding fluid flow rate used by MQL cooling and lubrication is very small, i.e., 50–200 mL/h, and a small amount of change will not result
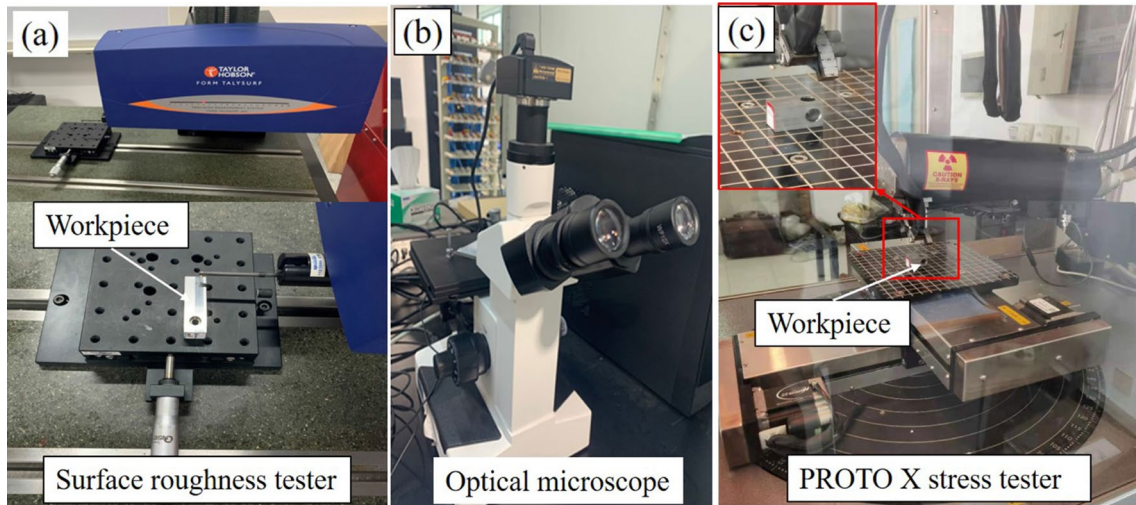

Fig. 8 Instruments used in surface quality detection. **a** Surface roughness, **b** surface morphology, **c** surface residual stress

Table 6 Parameters of related test instruments

| Objects	Detecting instrument	Testing parameters
Surface roughness	Form Talysurfi200 roughness tester	(a) Moving speed: 1 mm/s (b) Testing distance: 5 mm (c) Sampling interval: 0.125 μm
Surface morphology	9XF transmission reflection metallo-graphic microscope	(a) Magnification: 100 X (b) Testing area: 80 mm×50 mm
Surface residual stress	PROTO X ray stress detector	(a) Target: Cr (b) Elastic Modulus: − 98.6124 MPa/° (c) Bragg angle 2θ:156.31°
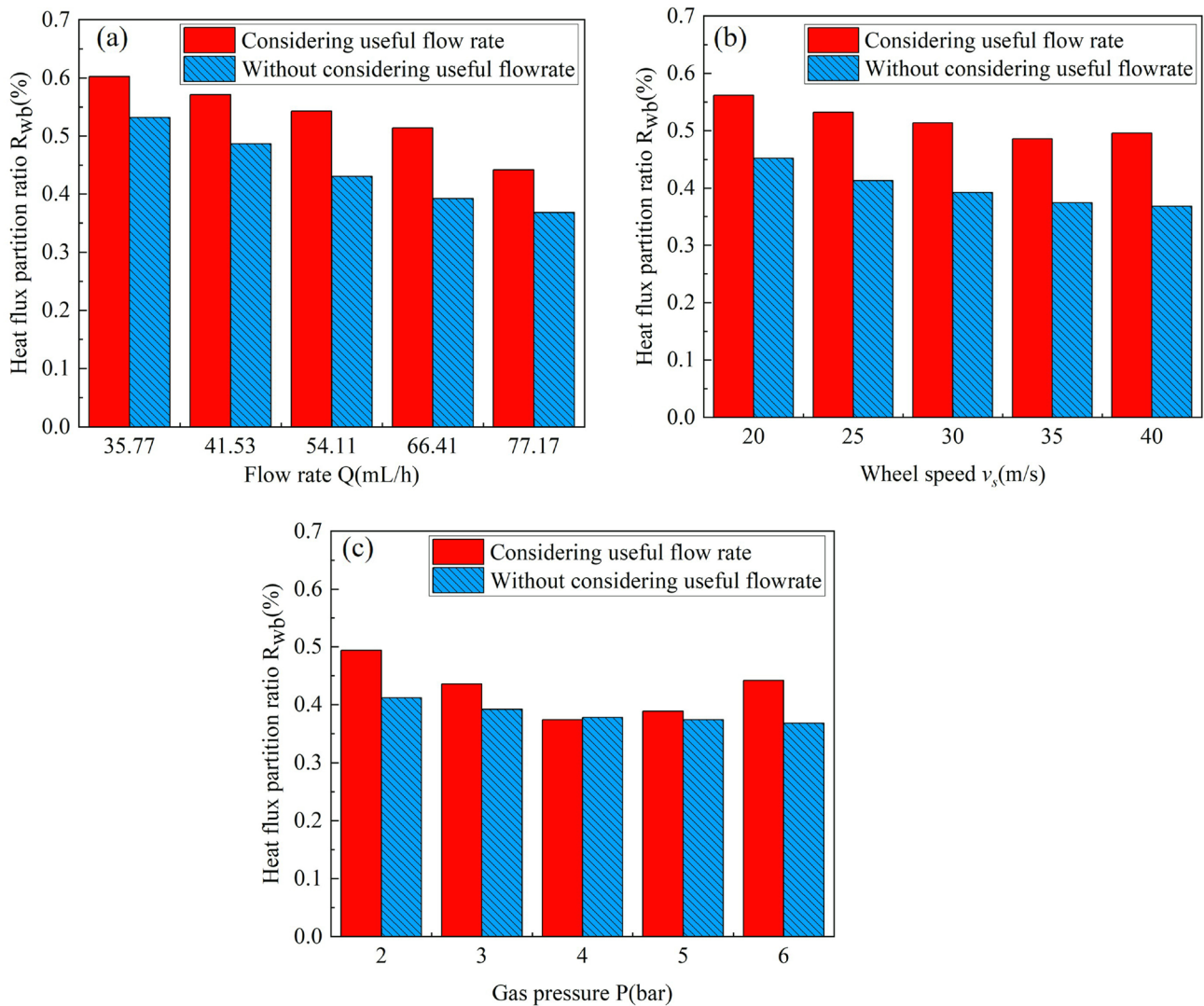
Fig. 9 Proportion of grinding heat participated to workpiece under **a** different flow rate, **b** different wheel speed, **c** different gas pressure

in a significant impact on the useful flow rate of the grinding fluid.

As shown in Fig. 10b, with the increase of the wheel speed, the useful flow rate of the grinding fluid first increases and then decreases. At high gas pressure, the kinetic energy of the grinding liquid droplets is large. When reaching the grinding area, the droplets collide with the wheel and workpiece before splashing, which reduces the useful flow rate. With the increase of the wheel speed, the strength of the air boundary layer in the flow field of the grinding wheel increases. The hindering effect on the droplets increases, resulting in the decrease of the droplet velocity, thereby reducing the splashing of the droplets against the wall, and increasing the useful flow rate. In the case that the wheel is too high, the air boundary is so strong that it makes the grinding fluid droplets more difficult to penetrate into the grinding zone. The useful flow rate of grinding fluid would decrease.

It can be seen from Fig. 10c that with the increase of the pressure, the useful flow rate first increases and then decreases. In the case that the gas pressure is low, it is difficult for the grinding fluid droplets at low speed to penetrate into the grinding zone. Thus, the useful flow rate is small. As the gas pressure increases, the droplets penetration ability is enhanced, which leads to the increase of grinding fluid useful flow rate. As the pressure continues to increase, when the pressure exceeds a certain value (4 bar), the velocity of the droplets becomes so high that the wall-impact splash phenomenon occurs, causing the useful flow rate to decrease.

The useful flow rate of grinding fluid into the grinding zone is mainly affected by the wheel speed, the flow of grinding fluid and the pressure of compressed air. Based on the wheel
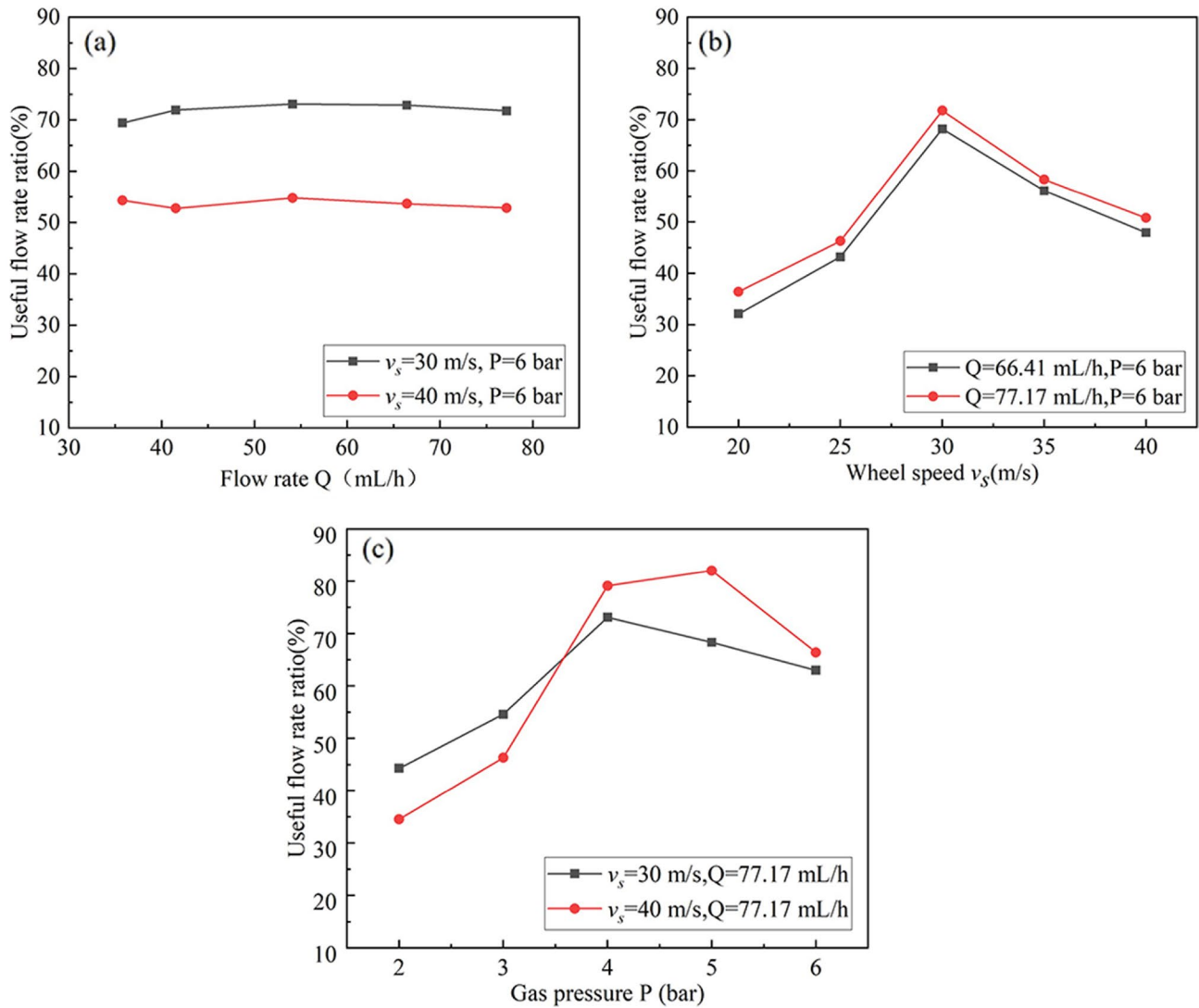
Fig. 10 Useful flow ratio under **a** different flow rate, **b** different wheel speed, **c** different gas pressure

speed, the grinding fluid flow rate and the compressed gas pressure have a complicated effect on the useful flow rate, and the function form cannot be directly determined. Therefore, the series is used for parameter fitting, and the function is performed according to the influence trend of each parameter on the useful flow rate. The final fitting form is expressed as follows:

$$\xi = \beta_1 + \beta_2 Q + \beta_3 v_s + \beta_4 P + \beta_5 v_s^2 + \beta_6 P^2 + \beta_7 Q^{\beta_8} \tag{25}$$

The values of the parameters of β_1, β_2, β_3, β_4, β_5, β_6, β_7 and β_8 in the grain size model are shown in Table 7. The units of wheel speed, gas pressure and grinding fluid flow rate are m/s, bar, and mL/h, respectively. For model verification, MQL grinding experiment was carried out with the experiment parameters shown in Table 8. The comparison between the experimental results and the calculated results is shown in Fig. 11, and the error is 5.67%.

Table 7 Useful flow rate fitting parameters of useful flow rate

β_1	β_2	β_3	β_4	β_5	β_6	β_7	β_8
− 14.566	− 0.112	2.5487	− 2.299	− 0.0004	− 0.0408	0.199	0.0253

Table 8 MQL grinding parameters, $v_w = 0.01$ m/s, $a_p = 8$ μm

	Wheel speed v_s [m/s]	Grinding fluid flow rate Q [mL/h]	Gas pressure P [bar]
1	20	66.41	6
2	25	77.17	6
3	30	77.17	2
4	35	66.41	4
5	40	66.41	6
6	40	77.17	6

Fig. 12 Comparison of experimental temperature and temperature model prediction results

Fig. 11 Comparison between experimental and calculated results of the useful flow ratio
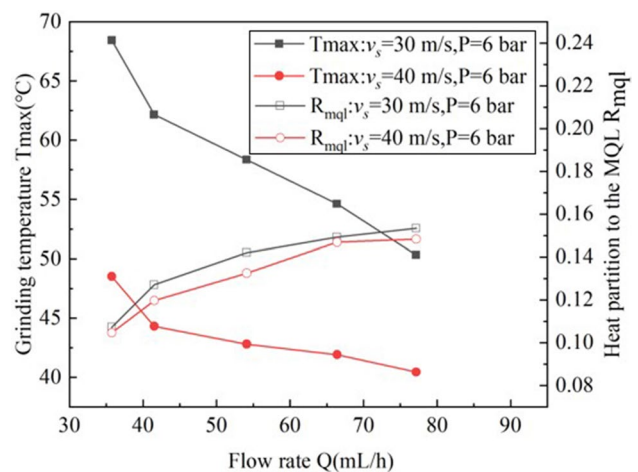
Fig. 13 Influence of flow rate on grinding temperature and heat partition to MQL jet

4.3 The Result of Grinding Temperature

The grinding temperature under different grinding conditions was calculated and compared with the temperature measured in the experiment (as shown in Fig. 12), and the error of the model calculation result is 9.45%. The parameters of experiment are shown in Table 8.

It can be seen from Fig. 12 that, compared with dry grinding, the grinding temperature under MQL grinding conditions is lower, and MQL shows a good cooling effect. On the contrary, compared with wet grinding, the grinding temperature under MQL condition is slightly higher, which is because that MQL grinding only has a small amount of grinding fluid, and the heat carried by the grinding fluid is less than that under wet grinding conditions. It can be found that with the increase of the wheel speed, the grinding temperature difference between MQL grinding and wet grinding is reduced. This is due to the fact that as the wheel speed increases, the air barrier is strengthened, thereby preventing the grinding fluid from entering the grinding zone. The MQL grinding fluid can still enter the grinding area due
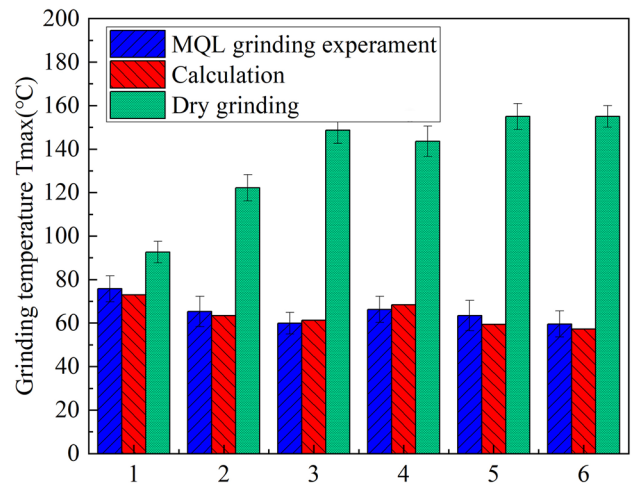
to its strong penetrating force, maintaining a good cooling effect. Therefore, MQL grinding is more suitable for high-speed grinding.

In this study, the grinding experiment was conducted under different conditions, and the grinding temperature was measured under different experimental conditions. Figures 13, 14, 15 show the changing trend of the grinding temperature and heat partition to MQL jet with the flow rate, the wheel speed, and the pressure of the compressed gas.

According to Fig. 13, when the grinding fluid flow rate is less than 45 mL/h, the grinding temperature tends to decrease with the increase of the grinding fluid flow rate; while at the grinding fluid flow rate greater than 45 mL/h, as the grinding fluid flow rate increases, the decreasing tendency of the grinding temperature is slowed down. Due to
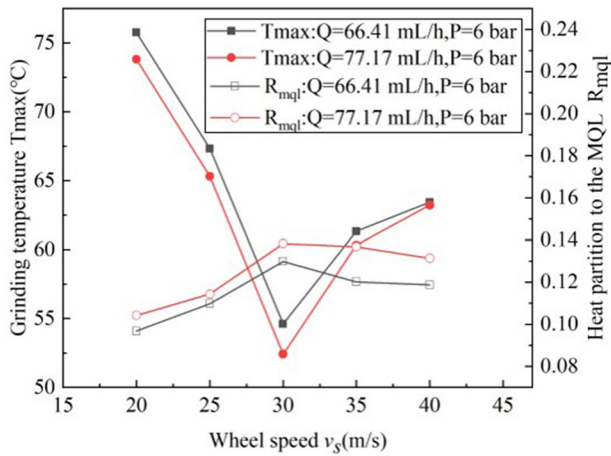
Fig. 14 Influence of wheel speed on grinding temperature and heat partition to MQL jet
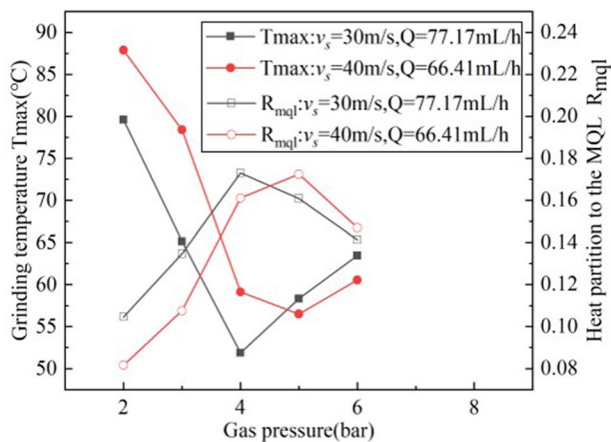

Fig. 15 Influence of gas pressure on grinding temperature and heat partition to MQL jet

the increase of the flow rate of the grinding fluid, the content of discrete items in the MQL jet continues to increase, resulting in a more intense energy exchange between the grinding fluid and the compressed air, thereby reducing the speed of the MQL jet. Under higher gas pressure, the increase of the grinding fluid flow rate can reduce the droplet velocity, and prevent the failure of the droplets to cool and lubricate due to splashing against the wall. Consequently, the heat partition to MQL jet increases, which lead to the decrease of grinding temperature. However, with the continuous increase of the grinding fluid flow rate, the droplet velocity becomes smaller, and the ability to penetrate the air boundary layer is reduced, slowing down in the downward trend of the grinding temperature.

As shown in Fig. 14, with the increase of wheel speed, the grinding temperature first decreases and then increases. As the wheel speed increases, the working abrasive grains

increase per unit time and the grinding thickness decreases. The deformation of the debris increases and the abrasive particles that produce plough and scratching effects increase, leading to the increase of grinding temperature. In the MQL grinding process, if the gas pressure is too high, the lubricant droplet velocity will be too high to be attached to the surface of the workpiece. As the wheel speed increases, the speed of the grinding fluid droplets is reduced because of the stronger air boundary. Besides, more lubricant droplets are attached to the workpiece, so that the useful flow rate of the grinding fluid is increased, and the heat partition to MQL jet increases. When the wheel speed increases to a certain value (30 m/s), the wheel speed will continue to increase, and the strength of the air boundary layer will become too strong, resulting in the reduction of the grinding fluid entering the grinding zone, which will eventually cause the decrease of the heat partition to MQL jet, and the increase of grinding temperature.

It can be found from Fig. 15 that, as the compressed gas pressure increases, the grinding temperature first decreases and then increases, meanwhile, at different wheel speeds, the inflection point of the temperature curve varies. Specifically, when the wheel speed reaches 30 m/s, the inflection point of gas pressure is 4 bar, and the grinding temperature reaches the lowest value; while at the grinding wheel speed of 40 m/s, the gas pressure is 5 bar, and the grinding temperature reaches the lowest value. With the increase of the compressed gas, the speed of the MQL jet increases, and the penetration ability of the grinding liquid droplets is enhanced, making it easier to pass through the air boundary layer and enter into the grinding area. As a result, the heat partition to MQL jet increases. In the case that the pressure reaches a certain critical value, the gas pressure continues to increase, and the speed of the lubricant droplets would be too high. The grinding fluid droplets collide with the surface of the workpiece and the grinding wheel, rebounding and splashing, which makes them unable to play the role of cooling and lubrication, resulting in the decrease of heat partition to MQL jet, and the increase of the surface grinding temperature of the workpiece.

5 Optimization Analysis of the Surface Quality

5.1 Effect on Surface Residual Stress

The residual stress on the surface of the workpiece will have an impact on the geometric shape and dimensional accuracy of the cost surface, as well as the fatigue strength of the workpiece, and further affect the performance and service life of the workpiece [35–38]. To study the influence of different MQL grinding parameters on, and better control the

residual stress on the surface of the workpiece, the MQL grinding experiments was conducted under different wheel speed, air pressure and flow rate.

The workpieces are subjected to thermal and mechanical loads during grinding which results in the generation of residual stress. With a fast cooling, the expansion of grinding surface layer is resisted by the subsequent unchanged volume in the depth, which results in compressive stress. It can be seen from Fig. 16 that the tangential and normal residual compressive stresses decrease with the increase of the grinding fluid flow rate. As the flow of lubricating fluid increases, both the grinding force and the grinding temperature decrease, but the grinding fluid flow rate shows a greater

influence on the grinding force, and the residual compressive stress caused by the grinding load decreases.

Figure 17 shows that with the increase of the wheel speed, the tangential and normal residual compressive stresses first increase and then decrease. At the wheel speed of less than 30 m/s, with the increase of the wheel speed, the MQL cooling effect increases, and the grinding temperature decreases. Consequently, the tensile stress caused by the grinding thermal load decreases, which in turn leads to an increase in the residual compressive stress. In the case that the wheel speed is higher than 30 m/s, the increase of the wheel speed will result in the increase of the strength of the air boundary layer, the decrease of the cooling effect of MQL, and
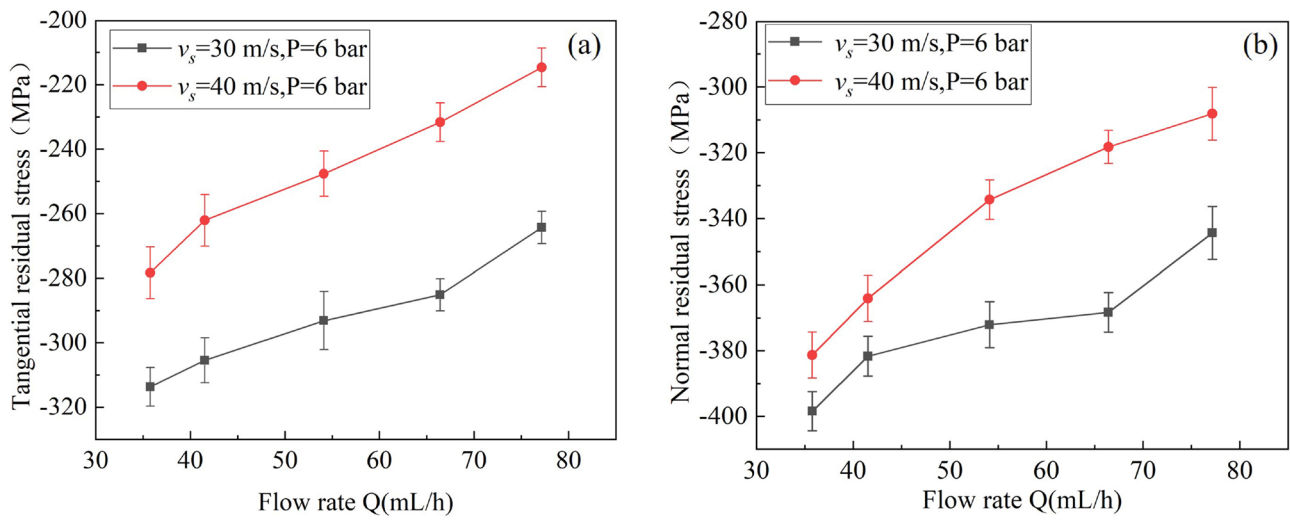

Fig. 16 Influence of grinding fluid flow on residual stress. **a** Tangential residual stress; **b** normal residual stress
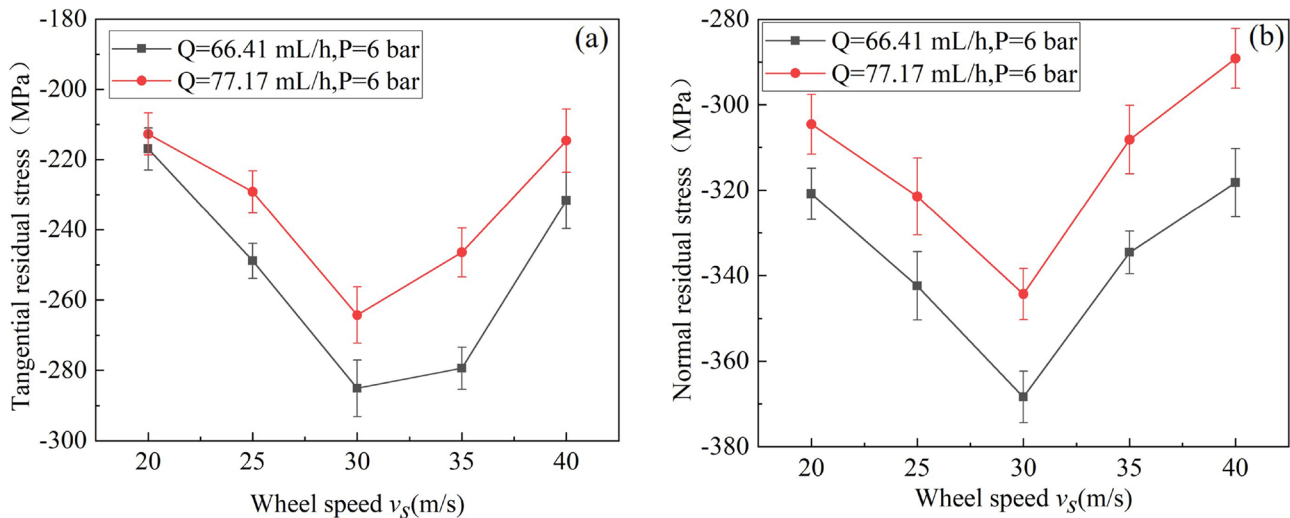

Fig. 17 Influence of wheel speed on residual stress. **a** Tangential residual stress; **b** normal residual stress

the rise of the grinding temperature. As a result, the tensile stress caused by the grinding thermal load increases, and the residual compressive stress on the surface of the workpiece decreases.

Figure 18 shows that, with the increase of compressed gas pressure, the tangential and normal residual compressive stresses first increase and then decrease. If the wheel speed is high, the compressed gas pressure will be increased, the cooling effect of MQL is enhanced, and both the grinding temperature and the tensile stress generated by the grinding thermal load are reduced. Besides, the residual compressive stress on the surface of the workpiece is increased. When the pressure exceeds a certain critical value (4 bar), the pressure continues to increase, resulting the reduction of cooling effect, the rise of grinding temperature, and the increase of the tensile stress caused by the grinding thermal load, which leads to the reduction of the residual compressive stress on the surface of the workpiece.

5.2 Effect on Surface Morphology

After grinding, the surface morphology of each workpiece was detected by using 9XF transmission reflection metallographic microscope under different grinding conditions. The image in Fig. 19 shows the surface morphology, and reveals that the parameters of MQL grinding have a great influence on the surface morphology of the workpiece. With the increased flow rate of lubricant, the grooves and pits on the surface decrease (Fig. 19a–c). Under low-gas-pressure condition, the pits on the surface are larger than those under high-gas-pressure condition (Fig. 19d, e). A comparison of Fig. 19c, f reveals that the change of wheel speed also has an impact on the surface morphology of the workpiece.

To further analyze the influence of different MQL grinding parameters on the surface morphology, the grinding tests with different parameter combinations were carried out, and the surface roughness of the workpiece was detected by using the Form Talysurfi 200 roughness meter with the result shown in Fig. 20.

According to Fig. 20a, with the increase of the lubricant flow rate, the surface roughness of the workpiece decreases, but the decreasing trend is relatively gentle. The increase of the grinding fluid flow rate will result in the increase of the grinding fluid entering the grinding zone, the improvement of the lubrication effect, as well as the reduction of grinding force, the plastic deformation of the surface material of the workpiece and the surface roughness. However, the amount of change in the flow rate of the grinding fluid in MQL grinding is small, and its effect on the improvement of lubrication conditions is limited. Therefore, the decreasing trend of the surface roughness is relatively gentle, and even when the flow rate of the grinding fluid increases to a certain extent, the surface roughness remains almost unimproved.

With the increase of the wheel speed, the surface roughness of the workpiece continues to decrease, and the trend of the decrease of the surface roughness continues to slow down, as shown in Fig. 20b. The increase of the wheel speed makes more abrasive particles participate in the grinding per unit time, consequently, the thickness of the grinding decreases, and the grinding force is reduced, which leads to the decrease of plastic deformation of the material of the workpiece, and the surface roughness of the workpiece is reduced [39, 40]. However, the increase of the wheel speed results in the increase of the hindering effect of the air boundary layer, the decrease of the grinding fluid entering the grinding zone, the deterioration of cooling and lubricating effect, and the rise of the grinding temperature, and
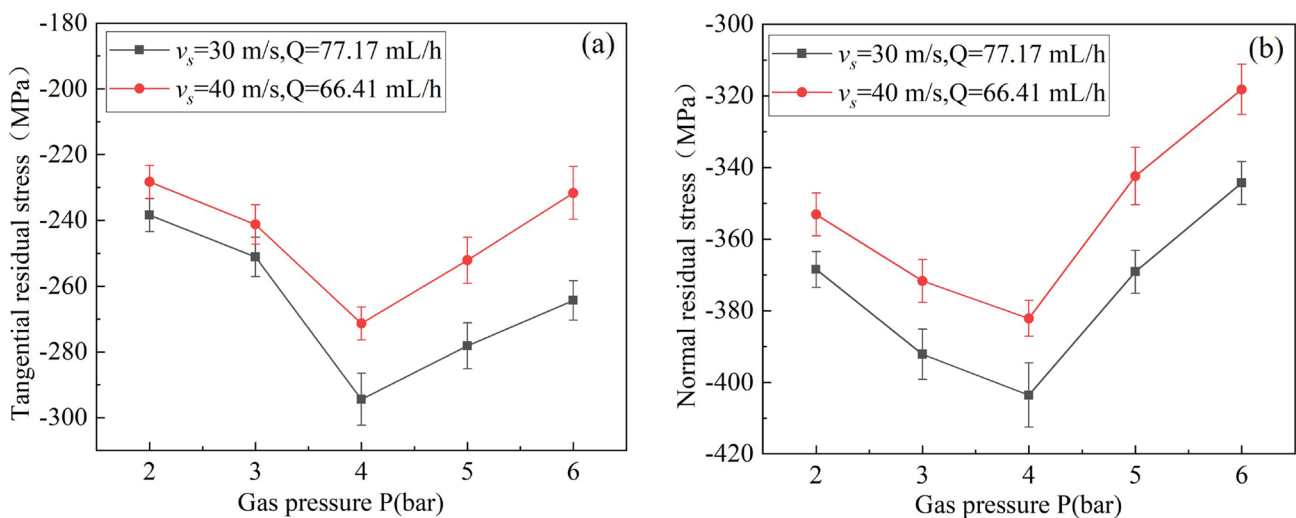

Fig. 18 Influence of gas pressure on residual stress. **a** Tangential residual stress; **b** normal residual stress
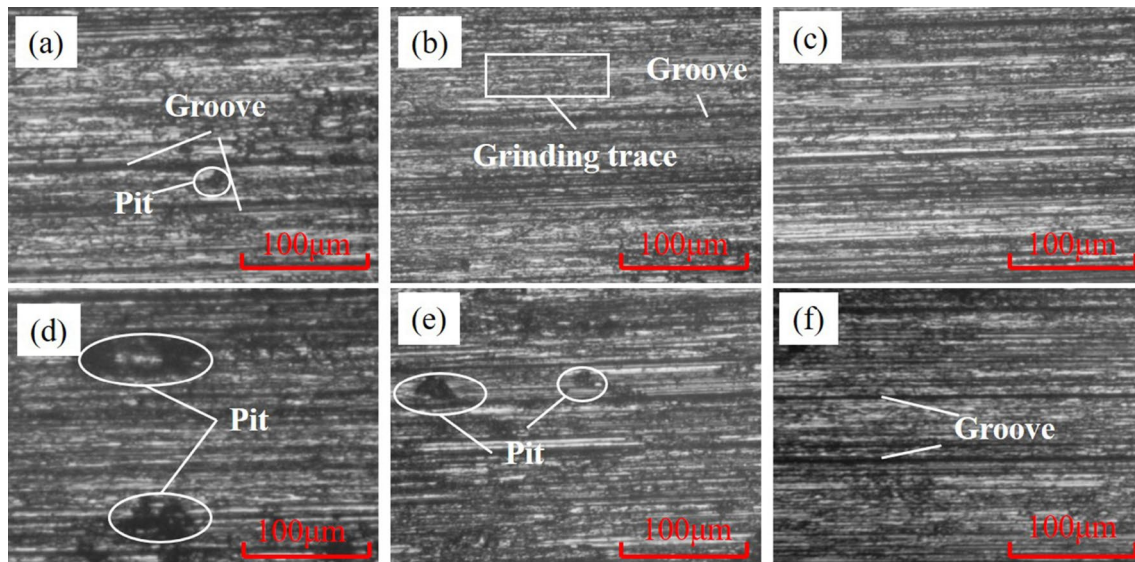
Fig. 19 Surface morphology under different parameters. **a** Q = 35.44 mL/h, v_s = 30 m/s; P = 4 bar; **b** Q = 54.44 mL/h, v_s = 30 m/s, P = 4 bar; **c** Q = 77.17 mL/h, v_s = 30 m/s, P = 4 bar; **d** Q = 54.44 mL/h, v_s = 30 m/s, P = 2 bar; **e** Q = 54.44 mL/h, v_s = 30 m/s, P = 4 bar; **f** Q = 77.17 mL/h, v_s = 40 m/s, P = 4 bar

eventually the increase of the plastic deformation of the workpiece surface material. In addition, the surface roughness of the workpiece increases.

It can be seen from Fig. 20c that as the gas pressure increases, the surface roughness of the workpiece first decreases and then increases, and the change trend is affected by the wheel speed. The higher the gas pressure, the higher the MQL jet velocity, and the more the grinding fluid entering the grinding zone. As a result, the cooling and lubricating effect is enhanced, the grinding force is reduced, and the grinding temperature is decreased, which in turn leads to a reduction in surface roughness. High MQL jet velocity will enhance the chip removal ability, and mitigate the damage to the machined surface by the wear debris. However, when the gas pressure exceeds a certain value, the effect of the increase of gas pressure on the reduction of the surface roughness decreases, and the surface roughness even increases. For example, if the grinding wheel linear velocity v_s = 30 m/s, and the gas pressure exceeds 5 bar, the surface roughness begins to increase; while when v_s = 40 m/s, if the gas pressure exceeds 4 bar, the roughness decrease trend begins to slow down.

6 Conclusions

In this study, the cooling performance of MQL grinding was studied by using theoretical modeling and experimental research, and the in-depth analysis of the mechanism of the influence of the MQL parameters on the cooling performance and the surface quality of the workpiece was conducted. According to the research, the following conclusions were drawn:

(1) The MQL grinding thermal analysis was carried out, and the grinding energy partition model and heat transfer model considering the useful flow rate of grinding fluid were established, which were verified by the maraging steel 3J33 grinding experiment. These models can be used for MQL grinding temperature prediction with the average error of 9.45%.

(2) Grinding wheel speed and gas pressure have a more significant influence on the useful flow rate of the grinding fluid. When improving the cooling performance of MQL grinding, the grinding wheel speed and gas pressure should be given priority. The grinding fluid flow rate has little influence on the useful flow rate of grinding fluid, but significant impact on the surface quality of the workpiece. As the grinding fluid flow rate increases, the surface quality is improved.

(3) In MQL grinding, the heat partition to MQL jet is available to be increased by changing the wheel speed, gas pressure and coolant flow rate reasonably. MQL grinding is more suitable for high-speed grinding. The MQL grinding fluid can enter the strengthened air barrier with the increase of the wheel speed due to its strong penetrating force. It has been proven that high wheel speed and critical pressure may lead to higher heat partition (17.2%) to MQL jet, which may lead to lower grinding temperature and better surface quality.

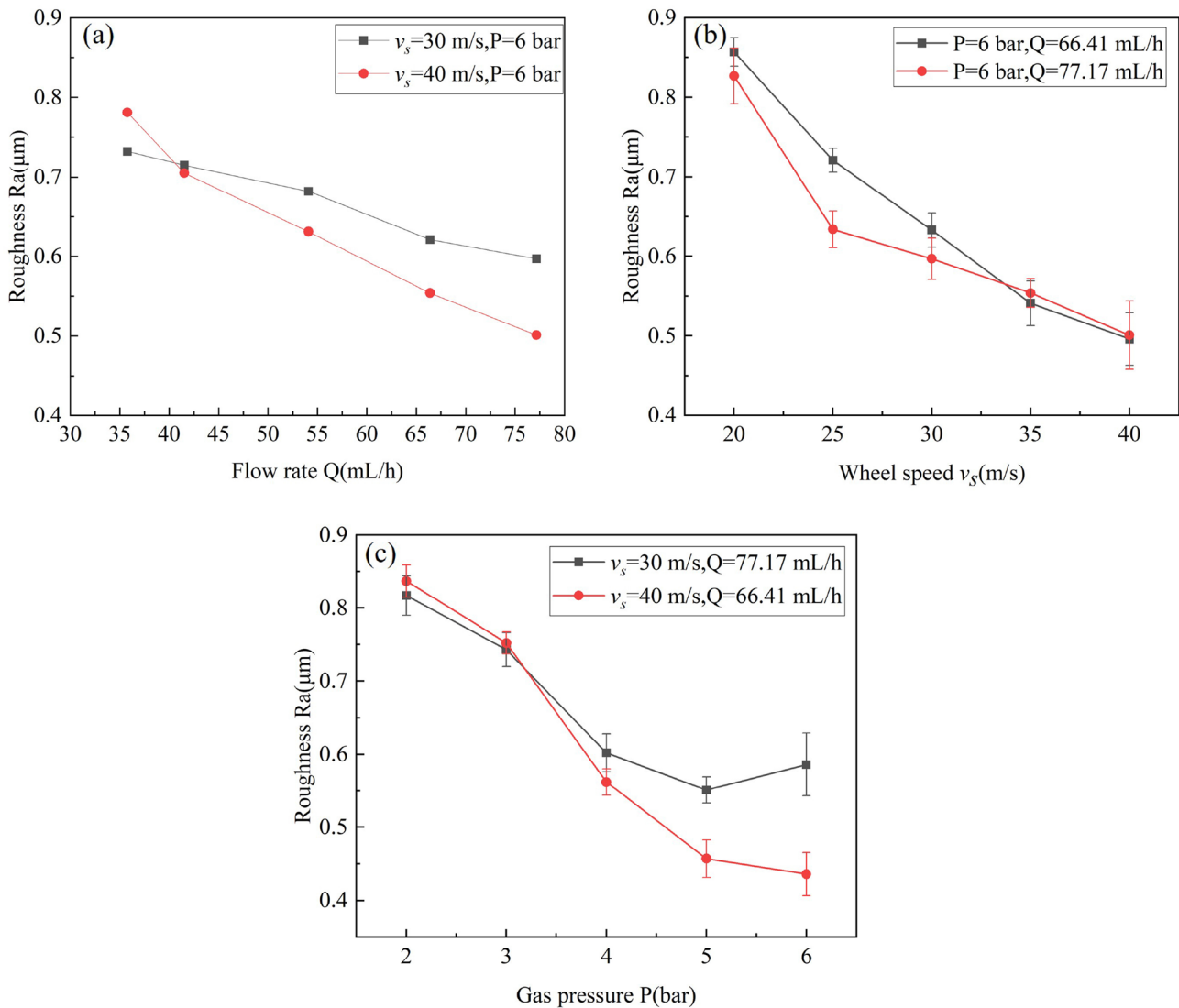(4) Grinding wheel speed, gas pressure and grinding fluid flow will all affect the surface quality of the workpiece.

Fig. 20 The effect of MQL grinding parameters on surface roughness: **a** flow rate **b** wheel speed, **c** gas pressure

With the increase of the flow rate of the grinding fluid, the surface quality of the workpiece is improved. The influence of grinding wheel speed and gas pressure on the surface quality of the workpiece is non-linear. If the wheel speed is constant, the gas pressure has a critical value. While when it is less than this value, the surface quality of the workpiece will be improved with the increase of the gas pressure. While when it is less than this value, it will decrease with the increase of the gas pressure.

Author contributions ZD: conceptualization; investigation; resources; methodology; writing—reviewing and editing; project administration; funding acquisition. JS: investigation; data curation; formal analysis; methodology; validation; writing—original draft; writing—reviewing and editing. WG: investigation; data curation; formal analysis; writing—reviewing and editing. XJ and CW: validation; resources. SYL: supervision.

Availability of data and materials Not applicable.

Code availability Not applicable.

Declarations

Conflict of interest On behalf of all authors, the corresponding author states that there is no conflict of interest.

References

1. Li, K. M., & Chou, S. Y. (2010). Experimental evaluation of minimum quantity lubrication in near micro-milling. *Journal of Materials Processing Technology, 210*(15), 2163–2170. https://doi.org/10.1016/j.jmatprotec.2010.07.031

2. Sun, C., Xiu, S., Hong, Y., Kong, X., & Lu, Y. (2021). Prediction on residual stress with mechanical-thermal and transformation coupled in DGH. *International Journal of Mechanical Sciences*. https://doi.org/10.1016/j.ijmecsci.2020.105629

3. Zhang, Y., Wang, Q., Li, C., Piao, Y., Hou, N., & Hu, K. (2021). Characterization of surface and subsurface defects induced by abrasive machining of optical crystals using grazing incidence X-ray diffraction and molecular dynamics. *Journal of Advanced Research*. https://doi.org/10.1016/j.jare.2021.05.006

4. Guo, W. C., Wu, C. J., Ding, Z. S., & Zhou, Q. Z. (2021). Prediction of surface roughness based on a hybrid feature selection method and long short-term memory network in grinding. *International Journal of Advanced Manufacturing Technology, 112*(9–10), 2853–2871. https://doi.org/10.1007/s00170-020-06523-z

5. Zhu, D. H., Feng, X. Z., Xu, X. H., Yang, Z. Y., Li, W. L., Yan, S. J., et al. (2020). Robotic grinding of complex components: A step towards efficient and intelligent machining-challenges, solutions, and applications. *Robotics and Computer-Integrated Manufacturing, 65*, 101908. https://doi.org/10.1016/j.rcim.2019.101908

6. Lopes, J. C., Fragoso, K. M., Garcia, M. V., Ribeiro, F. S. F., Francelin, A. P., Sanchez, L. E. D., et al. (2019). Behavior of hardened steel grinding using MQL under cold air and MQL CBN wheel cleaning. *International Journal of Advanced Manufacturing Technology, 105*(10), 4373–4387. https://doi.org/10.1007/s00170-019-04571-8

7. Yang, M., Li, C. H., Zhang, Y. B., Jia, D. Z., Zhang, X. P., Hou, Y. L., et al. (2017). Maximum undeformed equivalent chip thickness for ductile-brittle transition of zirconia ceramics under different lubrication conditions. *International Journal of Machine Tools and Manufacture, 122*, 41–51. https://doi.org/10.1016/j.ijmachtools.2017.06.003

8. Tawakoli, T., Hadad, M. J., & Sadeghi, M. H. (2010). Influence of oil mist parameters on minimum quantity lubrication—MQL grinding process. *International Journal of Machine Tools and Manufacture, 50*(6), 521–531. https://doi.org/10.1016/j.ijmachtools.2010.03.005

9. Jia, D. Z., Li, C. H., Zhang, D. K., Zhang, Y. B., & Zhang, X. W. (2014). Experimental verification of nanoparticle jet minimum quantity lubrication effectiveness in grinding. *Journal of Nanoparticle Research, 16*(12), 1–15. https://doi.org/10.1007/s11051-014-2758-7

10. Shao, Y. M., Fergani, O., Ding, Z. S., Li, B. Z., & Liang, S. Y. (2016). Experimental investigation of residual stress in minimum quantity lubrication grinding of AISI 1018 steel. *Journal of Manufacturing Science and Engineering-Transactions of the Asme, 138*(1), 711–718. https://doi.org/10.1115/1.4029956

11. Ding, Z., Li, B., Liang, S. Y., Ding, Z. S., Li, B. Z., & Liang, S. Y. (2015). Maraging steel phase transformation in high strain rate grinding. *International Journal of Advanced Manufacturing Technology, 80*(1–4), 711–718. https://doi.org/10.1007/s00170-015-7014-5

12. Zhuang, K., Fu, C., Weng, J., & Hu, C. (2021). Cutting edge microgeometries in metal cutting: A review. *The International Journal of Advanced Manufacturing Technology*. https://doi.org/10.1007/s00170-021-07558-6

13. Xiao, G., Song, K., He, Y., Wang, W., Zhang, Y., & Dai, W. (2021). Prediction and experimental research of abrasive belt grinding residual stress for titanium alloy based on analytical method. *The International Journal of Advanced Manufacturing Technology, 115*, 1111–1125. https://doi.org/10.1007/s00170-021-07272-3

14. Li, C., Li, X. L., Huang, S. Q., Li, L. Q., & Zhang, F. H. (2021). Ultra-precision grinding of Gd3Ga5O12 crystals with graphene oxide grinding fluid: Material deformation mechanism and performance evaluation. *Journal of Manufacturing Processes, 61*, 417–427. https://doi.org/10.1016/j.jmapro.2020.11.037

15. Sun, C., Duan, J. C., Lan, D. X., Liu, Z. X., & Xiu, S. C. (2018). Prediction about ground hardening layers distribution on grinding chatter by contact stiffness. *Archives of Civil and Mechanical Engineering, 18*(4), 1626–1642. https://doi.org/10.1016/j.acme.2018.06.010

16. Xi, X. X., Zhu, Y. J., Chen, T., Wu, Z. X., Angge, I. L., & Ding, W. F. (2021). Surface burn behavior in creep-feed deep grinding of gamma titanium aluminide intermetallic: characterization, mechanism, and effects. *International Journal of Advanced Manufacturing Technology, 113*(3–4), 985–996. https://doi.org/10.1007/s00170-021-06677-4

17. Ji, X., Li, B. Z., Zhang, X. P., & Liang, S. Y. (2014). The effects of minimum quantity lubrication (MQL) on machining force, temperature, and residual stress. *International Journal of Precision Engineering and Manufacturing, 15*(11), 2443–2451. https://doi.org/10.1007/s12541-014-0612-6

18. Balan, A. S. S., Vijayaraghavan, L., & Krishnamurthy, R. (2013). Minimum quantity lubricated grinding of Inconel 751 alloy. *Materials and Manufacturing Processes, 28*(4), 430–435. https://doi.org/10.1080/10426914.2013.763965

19. Liao, Y. S., Liao, C. H., & Lin, H. M. (2017). Study of oil-water ratio and flow rate of MQL fluid in high speed milling of Inconel 718. *International Journal of Precision Engineering and Manufacturing, 18*(2), 257–262. https://doi.org/10.1007/s12541-017-0033-4

20. Huang, X. M., Ren, Y. H., Li, T., Zhou, Z. X., & Zhang, G. F. (2018). Influence of minimum quantity lubrication parameters on grind-hardening process. *Materials and Manufacturing Processes, 33*(1), 69–76. https://doi.org/10.1080/10426914.2016.1269916

21. Balan, A. S. S., Kullarwar, T., Vijayaraghavan, L., & Krishnamurthy, R. (2017). Computational fluid dynamics analysis of MQL spray parameters and its influence on superalloy grinding. *Machining Science and Technology, 21*(4), 603–616. https://doi.org/10.1080/10910344.2017.1365889

22. Silva, L. R., Correa, E. C. S., Brandao, J. R., & De Avila, R. F. (2020). Environmentally friendly manufacturing: Behavior analysis of minimum quantity of lubricant—MQL in grinding process. *Journal of Cleaner Production*. https://doi.org/10.1016/j.jclepro.2013.01.033

23. Sun, Y., Su, Z., Gong, Y., Ba, D., Yin, G., Zhang, H., & Zhou, L. (2021). Analytical and experimental study on micro-grinding surface-generated mechanism of DD5 single-crystal superalloy using micro-diamond pencil grinding tool. *Archives of Civil and Mechanical Engineering, 21*(1), 1–22. https://doi.org/10.1007/s43452-020-00163-6

24. Liu, H., Song, W. Q., Niu, Y. H., & Zio, E. (2021). Generalized cauchy method for remaining useful life prediction of wind turbine gearboxes. *Mechanical Systems and Signal Processing, 153*(15), 107471. https://doi.org/10.1016/j.ymssp.2020.107471

25. Yang, M., Li, C. H., Zhang, Y. B., Wang, Y. G., Li, B. K., Jia, D. Z., et al. (2017). Research on microscale skull grinding

temperature field under different cooling conditions. *Applied Thermal Engineering, 126*, 525–537. https://doi.org/10.1016/j.applthermaleng.2017.07.183

26. Jamshidi, H., & Budak, E. (2018). Grinding temperature modeling based on a time dependent heat source. *8th Cirp Conference on High Performance Cutting (Hpc 2018), 77*, 299–302. https://doi.org/10.1016/j.procir.2018.09.020

27. Ding, Z. S., Jiang, X. H., Guo, M. X., & Liang, S. Y. (2018). Investigation of the grinding temperature and energy partition during cylindrical grinding. *International Journal of Advanced Manufacturing Technology, 97*(5–8), 1767–1778. https://doi.org/10.1007/s00170-018-1900-6

28. Sharmin, I., Moon, M., Talukder, S., Alam, M., & Ahmed, M. F. (2021). Impact of nozzle design on grinding temperature of hardened steel under MQL condition. *Materials Today-Proceedings, 38*, 3232–3237. https://doi.org/10.1016/j.matpr.2020.09.717

29. Li, B. K., Li, C. H., Zhang, Y. B., Wang, Y. G., Jia, D. Z., & Min, Y. (2016). Grinding temperature and energy ratio coefficient in MQL grinding of high-temperature nickel-base alloy by using different vegetable oils as base oil. *Chinese Journal of Aeronautics, 29*(4), 1084–1095. https://doi.org/10.1016/j.cja.2015.10.012

30. Wang, Y. G., Li, C. H., Zhang, Y. B., Yang, M., Li, B. K., Jia, D. Z., et al. (2016). Experimental evaluation of the lubrication properties of the wheel/workpiece interface in minimum quantity lubrication (MQL) grinding using different types of vegetable oils. *Journal of Cleaner Production, 127*, 487–499. https://doi.org/10.1016/j.jclepro.2016.03.121

31. Zhang, Y. B., Li, C. H., Jia, D. Z., Zhang, D. K., & Zhang, X. W. (2015). Experimental evaluation of MoS2 nanoparticles in jet MQL grinding with different types of vegetable oil as base oil. *Journal of Cleaner Production, 87*, 930–940. https://doi.org/10.1016/j.jclepro.2014.10.027

32. Hadad, M., & Sadeghi, B. (2012). Thermal analysis of minimum quantity lubrication-MQL grinding process. *International Journal of Machine Tools & Manufacture, 63*, 1–15. https://doi.org/10.1016/j.jclepro.2014.10.027

33. Kim, H. J., Kim, N. K., & Kwak, J. S. (2006). Heat flux distribution model by sequential algorithm of inverse heat transfer for determining workpiece temperature in creep feed grinding. *International Journal of Machine Tools and Manufacture, 46*(15), 2086–2093. https://doi.org/10.1016/j.ijmachtools.2005.12.007

34. Guo, C., & Malkin, S. (1992). First international conference on transport phenomena in processing. *Heat transfer in grinding*. (pp. 377). Technomic Publishing Company Inc

35. Sai, S. S., Manojkumar, K., & Ghosh, A. (2015). Assessment of spray quality from an external mix nozzle and its impact on SQL grinding performance. *International Journal of Machine Tools and Manufacture, 89*, 132–141. https://doi.org/10.1016/j.ijmachtools.2014.10.004

36. Hadad, M. J., Tawakoli, T., Sadeghi, M. H., & Sadeghi, B. (2012). Temperature and energy partition in minimum quantity lubrication-MQL grinding process. *International Journal of Machine Tools and Manufacture, 54–55*, 10–17. https://doi.org/10.1016/j.ijmachtools.2011.11.010

37. Ding, Z. S., Sun, G. X., Guo, M. X., Jiang, X. H., Li, B. Z., & Liang, S. Y. (2020). Effect of phase transition on micro-grinding-induced residual stress. *Journal of Materials Processing Technology, 281*, 116647. https://doi.org/10.1016/j.jmatprotec.2020.116647

38. Zhao, M., Mao, J., Ji, X., Feng, Y. X., & Liang, S. Y. (2021). Effect of crystallographic orientation on residual stress induced in micro-grinding. *International Journal of Advanced Manufacturing Technology, 112*(5–6), 1271–1284. https://doi.org/10.1007/s00170-020-06329-z

39. Jiang, X. H., Kong, X. J., Zhang, Z. Y., Wu, Z. P., Ding, Z. S., & Guo, M. X. (2020). Modeling the effects of Undeformed Chip Volume (UCV) on residual stresses during the milling of curved thin-walled parts. *International Journal of Mechanical Sciences*. https://doi.org/10.1016/j.ijmecsci.2019.105162

40. Wu, C. J., Pang, J. Z., Li, B. Z., & Liang, S. Y. (2019). High-speed grinding of HIP-SiC ceramics on transformation of microscopic features. *International Journal of Advanced Manufacturing Technology, 102*(5–8), 1913–1921. https://doi.org/10.1007/s00170-018-03226-4

Zishan Ding is an associate professor at University of Shanghai for Science and Technology. She received her doctorate from the Donghua University. She has been a visiting scholar in the Georgia Institute of Technology. She is senior member of China Society of Mechanical Engineering. Her research interests include grinding mechanism, grinding residual stress and grinding processing. She has previously completed the projects including National Natural Science Foundation of China and has published over 30 research articles in international journals.

Jian Sun is a graduate student at University of Shanghai for Science and Technology. His main direction of scientific activity is cutting mechanism of hard-to-machine materials in grinding. His current research interests include green manufacturing and intelligent manufacturing.

Weicheng Guo is a lecturer at University of Shanghai for Science and Technology. He was also a visiting scholar in Purdue University. His current research interests include precision machining of aerospace difficult-to-cut materials and intelligent manufacturing. He is a senior member of the Chinese Mechanical Engineering Society. He has anticipated and obtained several National Natural Science Foundation of China and has published over 20 international journal articles.

Xiaohui Jiang is an associate professor at University of Shanghai for Science and Technology. He received his doctorate from the Donghua University. As a visiting scholar, research in the Ohio State university, USA. He is senior member of China Society of Mechanical Engineering and member of the Expert Technical Committee of Shanghai Complex Metal Parts Additive Manufacturing Technology Center. His research interests include High-speed machining & Additive manufacturing & Intelligence manufacturing. He has has published over 30 research articles in international journals.

Steven Y. Liang is Morris M. Bryan, Jr. Professor in Mechanical Engineering for Advanced Manufacturing Systems at Georgia Institute of Technology, USA. Dr. Liang's research interests focus on precision manufacturing processes in the context of modeling, monitoring, control, and optimization. Dr. Liang's research program has been sponsored largely by federal agencies, national laboratories, along with industry sectors of aerospace, automotive, and energy to provide fundamental science and engineering with tangible application relevance. He has published over 200 scientific papers in recent 3 years.

Chongjun Wu is an associate professor in Donghua University. He's been working on high speed grinding mechanism of hard-to-machine materials for ten years, with more than 20 published journal articles and 300 citations. He is also an active member of the Chinese mechanical engineering society national abrasive technology committee. He also serves as an editor of Chinese journal "Diamond and Abrasives Engineering".